Hue University Journal of Science: Agriculture and Rural Development
pISSN: 2588-1191; eISSN: 2615-9708
Vol. 132, No. 3C, 2023, P. 37–49, DOI: 10.26459/hueunijard.v132i3C.7219

EVALUATION AND PREDICTION OF LAND USE, AND LAND COVER CHANGES USING REMOTE SENSING AND CA-ANN MODEL IN HUONG HOA DISTRICT, QUANG TRI PROVINCE

Nguyen Thuy Phuong[1] *, Nguyen Phuc Khoa[1], Le Thai Hung[1], Pham Gia Tung[2], Le Dinh Huy[1], Nguyen Trung Hai[1], Trinh Ngan Ha[1], Nguyen Huu Ngu[1], Tran Thanh Duc[1]

[1] University of Agriculture and Forestry, Hue University, 102 Phung Hung St., Hue, Vietnam
[2] International School – Hue University, 1 Dien Bien Phu St., Hue, Vietnam

* Correspondence to Nguyen Thuy Phuong <ntphuong.huaf@hueuni.edu.vn>
(*Received: May 26, 2022; Accepted: August 9, 2023*)

Abstract. Evaluation of land use and land cover change (LULC) is necessary for densely vegetated areas like Huong Hoa district, Quang Tri province. It is a basis for sustainable development strategies. Therefore, the study aims to evaluate the LULC change in the 10-year period of 2013–2023 by using Landsat 8 satellite image data with the Maximum Likelihood Classification method and to predict future LULC changes. The LULC maps for 2013, 2018, and 2023 are accurate, with Kappa coefficients of 0.82–0.85. In the period of 2013–2023, the dense vegetation area tended to decrease by 1.4%. The decrease was mainly due to the transition to sparse vegetation cover. Bare land increased by 0.5%, and the built-up area decreased by 0.6%. Meanwhile, the water bodies changed slightly. The prediction of LULC change with the CA-ANN model in the QGIS MOLUSCE plugin is based on the history of LULC change and two spatial variables: DEM and distance to the road. The accuracy of the CA-ANN model is satisfactory, with an overall accuracy of 86% and a Kappa coefficient of 0.76. In the simulated LULC of 2033, dense vegetation is predicted to keep a higher decrease (2%) in the area compared with the LULC of 2023. Sparse vegetation steadily increased by 1.3% over the subsequent 10 years. Similarly, the built-up area, water boddies, and bare land extended slightly by 0.5, 0.1, and 0.1%, respectively. The CA-ANN model in the QGIS MOLUSCE plugin is suitable for the simulated LULC changes for the studied area.

Keywords: LULC change, remote sensing, CA-ANN, LULC prediction

1 Introduction

The world's development has significantly altered land use and land cover (LULC) over the past two decades [1]. Land cover is defined as consisting of vegetation, water, soil, and other physical features created by human activities. Land use refers to the purpose that land serves, such as agriculture, residential land, wildlife habitat, and recreational land [2]. Land use and land cover monitoring helps develop strategies to balance conservation, use conflicts, and development pressures. Land use and land cover changes result mainly from urbanization, deforestation, and agricultural intensification [1]. Numerous studies provide clear evidence that the LULC changes affect climate change, soil quality, and the air environment [1, 3, 4]. Therefore, LULC change

monitoring is essential for sustainable natural resource management, environmental protection, agricultural planning, and food security.

Remote sensing techniques combined with Geographic Information Systems (GIS) have made mapping LULC easier than ever [5]. High-spatial-resolution satellite imagery and advanced image processing GIS technology have facilitated LULC monitoring and modelling [1]. There are three methods for the classification of LULC maps using remote sensing images, namely supervised classification, unsupervised classification, and object-based image analysis [6]. The supervised classification Maximum Likelihood Classifier (MLC) is widely applied in object identification and LULC classification [7, 8]. Mishra et al. compare MLC and MDC (Minimum Distance Classifier) methods. The results reveal that the MLC method has an overall accuracy of 79.2%, slightly higher than the MDC method of 74.9% [9]. Similarly, Norovsuren et al. and Seyam et al. use the MLC method to obtain a very high accuracy with the Kappa coefficient from 0.87 to 0.9 [10, 11].

There are some LULC predicted models, such as Markov chain, Cellular Automata, CLUE, and Land Change Model, that have been developed in recent times. The modules of Land Use Change Evaluation (MOLUSCE) are programmed by using Cellular Automata (CA) and Artificial Neutral Network (ANN) on QGIS software that can estimate the potential for LULC changes [12]. The CA-ANN model in MOLUSCE is a reliable tool for simulating LULC changes. Four algorithms are used in MOLUSCE: artificial neural network (ANN), logistic regression, multi-criteria evaluation, and weighting of evidence.

In this study, we mapped and evaluated LULC changes in Huong Hoa district, Quang Tri province, over a period of 10 years based on Landsat 8 satellite image data processed on ArcGIS software. On that basis, we carried out the simulation of the LULC change for 2033 using the QGIS MOLUSCE plugin.

2 Materials and methods

2.1 Study area

Huong Hoa is a mountainous district in western Quang Tri province. This area is influenced by the tropical monsoon regime and has its own characteristics of a sub-region of monsoon temperature and continental climate at the top of the Truong Son mountains. The annual average temperature is 22.5 °C, with the highest temperature of 38.2 °C and the lowest of 7.7 °C. The average rainfall is 1850 mm/year; the rainfall is concentrated from May to November, accounting for 88% of the annual rainfall, and the largest concentration is in September and October [13].

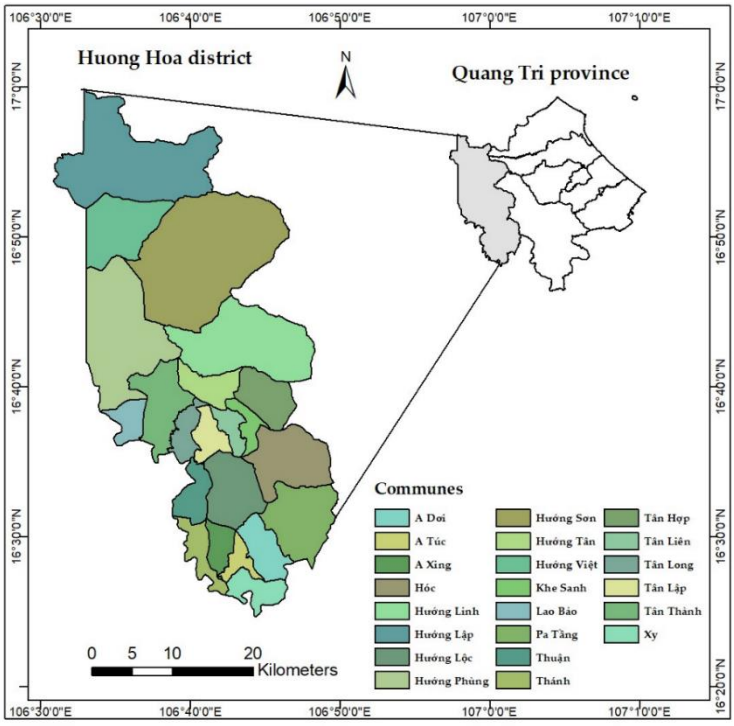

Fig. 1. Location map of the study area

2.2 Data collection

Landsat 8 OLI satellite image data were downloaded from the United States Geological Survey (USGS) (https://earthexplorer.usgs.gov/) at three-time points in 2013 (08/10/2013), 2018 (22/04/2018) and 2023 (14/01/2023) for LULC maps. The satellite image of the studied area was assembled from two pieces: 125/048 and 125/049 (path/row), with a combination of image channels from B1 to B7 in the WGS84 coordinate system. The image resolution is 30 × 30 m and had a cloud coverage of less than 10%, which helped to limit errors in interpreting.

Digital elevation model (DEM) data were downloaded from the USGS Earth Explorer at SRTM 1-ArcSecond Global (downloaded on 15/3/3023). The DEM data were resampled with the Raster processing tool in ArcMap to transfer to a resolution of 30 × 30 m. Road system data were collected from OpenStreetMap (14/05/2023) and classified distance from the road map. Satellite image data, DEM and distance from road data were processed, analysed, and mapped on ArcMap 10.8 software over the past 10 years.

2.3 LULC change map

The algorithm in MLC is based on two principles: the cells in each class have a normal distribution and decision following the Bayes theorem [14]. In MLC classification, the pixel with the highest probability is classified into the more appropriate class [15]. This method obtains the mean and variance of training samples computed for these samples. The MLC method has the following steps [16]: (1) image preprocessing, (2) initializing the number of classes and training parameters, and (3) running the MLC algorithm.

In this study, LULC was classified into five covers: Dense vegetation, Sparse vegetation, Built-up area, Water bodies, and Bare land.

The LULC maps built from satellite image interpretation has a certain error, so it is necessary to provide a reliable level of the LULC map. We randomly selected 150 points on each map with the Segmentation and Classification tool on ArcMap. In this study, the results were referenced with Google Earth images that superseded field observations. The error matrix was created to calculate the Kappa coefficient. This matrix provided overall accuracy, user accuracy (positive error), manufacturer accuracy (negative error), and Kappa coefficient, as shown in the studies of ESRI and Leta et al. [17, 18]. According to Xiong et al., if Kappa > 0.75, the LULC map has good accuracy [19].

The LULC change maps for the periods 2013–2018, 2018–2023, and 2013–2023 were built according to the following steps: (1) converting Raster map data to Polygon, (2) dissolving for each type of LULC, (3) intersetting two types of dissolved LULC maps, and (4) calculating the area change of each LULC.

2.4 Prediction of LULC change

The MOLUSCE Plugin in QGIS 2.8.9 software was used to analyse and model the future LULC change. This tool helps to evaluate the total area of change at the land cover level, simulate the change dynamically, and validate the model. This forecasting model is performed in four steps [20]:

(1) Change analysis and potential modelling: simulating the LULC model to estimate spatial changes and calculate LULC transition in the period 2013–2018. The transition matrix and change probabilities matrix were generated. Explanatory variables, including DEM data and distances to roads, can influence LULC variation.

(2) Forecasting and validating the simulated LULC model for 2023: The CA-ANN algorithm in the MOLUSCE plugin was used for transformation potential modelling and simulation. Based on the LULC change of 2013–2018 and explanatory variables, we built the

LULC simulation map for 2023. We compared the accuracy of the simulated LULC map for 2023 with the real LULC map for 2023 through the Kappa coefficient.

(3) Simulating the LULC map for 2033: We used the 10-year LULC change map (2013–2023) to simulate the LULC map for 2033.

(4) Calculating the rate of change of each LULC type for each period

$$\Delta\ (\%) = \frac{F_y - I_y}{S} \times 100 \quad (1)$$

where Δ is the rate of area change; I_y and F_y are the area of the first year and the last year; S is the total of the study area.

3 Results and discussion

3.1 LULC change

In this research, we built three LULC maps for 2013, 2018, and 2023 (Fig. 2) with the MLC method. There were five LULC classes, namely Dense vegetation, Sparse vegetation, Built-up area, Water bodies, and Bare land. The accuracy of the LULC maps was very good, with the overall accuracies of 89.3–91.3% and the Kappa coefficient of 0.82–0.85. These overall accuracies were slightly higher than those of Norovsuren et al. [10], with 86.5 and 89.0%. The Kappa coefficients were also higher than those of Abbas and Jaber, with 0.8 [21] and Mishra et al., with 0.76. Therefore, the LULC maps built from the Landsat 8 satellite images with the MLC method were suitable for LULC change evaluation [9].

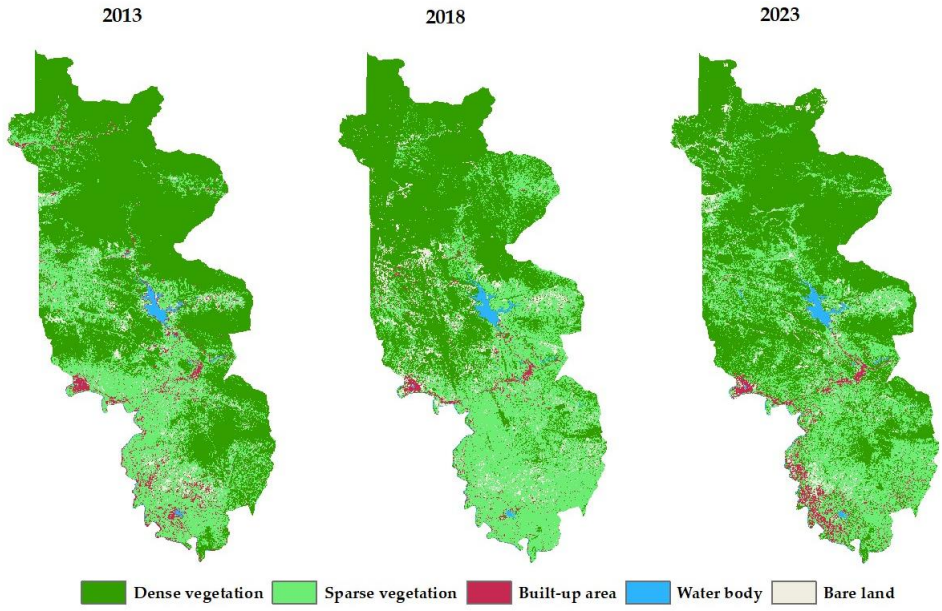

Fig. 2. LULC maps for 2013, 2018, and 2023

The statistical areas for LULC types are shown in Table 1. The total area of Huong Hoa district is approximately 1,151.8 km², most of which is covered with Dense and Sparse vegetation, accounting for 91.5%. This result is approximately equal to the district's agricultural land of 94.8% [22]. The Built-up area and Bare land have significant fluctuations from 2 to 4% and from 3.5 to 5.4% in the last 10 years. The Water bodies' area was stable, with 0.9–1.1%. This small change is due to increasing stream water level caused by rain.

In 2018, there was a significant reduction of 4.3 ha in the area of Dense vegetation, mainly converted by Sparse vegetation. The Bare land also increased significantly by 1.9 hectares. However, by 2023, this negative change trend has partially improved. The Dense vegetation land extended again by 2.9 ha, and Bare land decreased by 1.3 ha (Fig. 3).

Table 1. LULC area for 2013 and 2023

LULC	2013	2023	Δ	2013%	2023%	Δ%
Dense vegetation	699.1	682.8	-16.3	60.7	59.3	-1.4
Sparse vegetation	354.5	369.6	15.1	30.8	32.1	1.3
Built-up area	46.6	39.8	-6.7	4.0	3.5	-0.6
Water bodies	10.8	12.8	2.0	0.9	1.1	0.2
Bare land	40.9	46.8	5.9	3.5	4.1	0.5

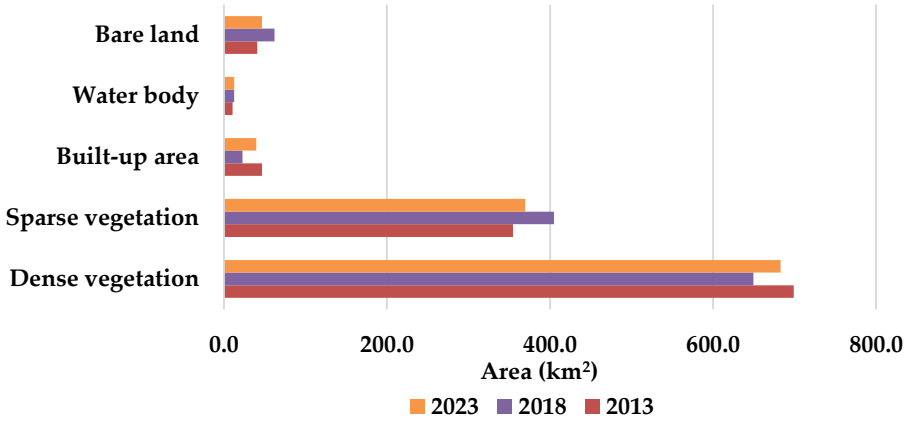

Fig. 3. LULC area in 2013, 2018, and 2023

Over the 10-year period of 2013–2023, 81.7% of the Dense vegetation area remained unchanged. Besides, its area decreased by 1.4%. This decrease was due to transferring to Sparse vegetation (6.4%) and Bare land (1.6%). For Sparse vegetation, 59.2% of the area remained stable. Its area increased by 1.3% due to becoming denser after 10 years. Harvesting plantation forests caused a decrease in area. However, this decrease was lower than the increase from Dense vegetation with 28.6%. The Built-up area changed differently, with only a third of the area remaining the same. Meanwhile, 37.3 and 20.5% were transferred from Sparse vegetation and Bare land. For Water bodies, 90.4% stayed unchanged and 0.2% slightly increased compared with 2013. Under different rainfall conditions, the water level increased in the streams and lakes, making an increase in the Water bodies and reducing Bare land by 6.7%. In general, Dense vegetation areas tended to decrease and Sparse vegetation tended to increase over the mentioned 10-year period. The remaining LULC classes changed slightly. Detailed information about LULC changes can be seen in Fig. 4.

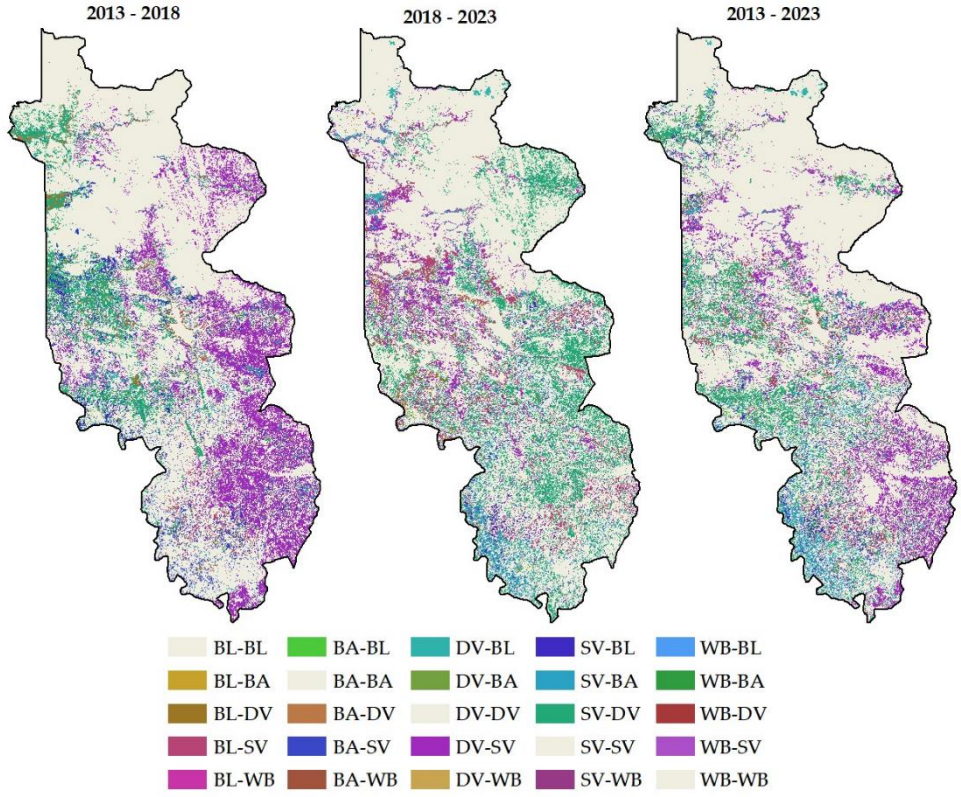

Fig. 4. LULC change map for periods 2013–2018, 2018–2023, and 2013–2023

(DV: Dense vegetation; SV: Sparse vegetation; BA: Built-up area; WB: Water bodies; BL: Bare land)

Table 2. Transition matrix between 2013 and 2023

LULC	Dense vegetation	Sparse vegetation	Built-up area	Water bodies	Bare land
Dense vegetation	0.817	0.164	0.002	0.000	0.016
Sparse vegetation	0.286	0.592	0.068	0.001	0.053
Built-up area	0.091	0.373	0.277	0.053	0.205
Water bodies	0.012	0.010	0.007	0.904	0.067
Bare land	0.145	0.664	0.029	0.004	0.157

3.3 Prediction of LULC map

We combined the history of LULC change with spatial variables: DEM data and distance to roads (Fig. 5). The CA-ANN algorithm in the MOLUSCE plugin was used to run the simulation LULC models for 2033. First, LULC changes data in the period 2013–2018 were used as a basis for

building a simulated LULC map for 2023 (Simulated 2023). This map was compared with the LULC map for 2023 by using remote sensing to determine the accuracy of the simulated LULC map for 2033 (Simulated 2033).

The simulated LULC map for 2023 had an overall accuracy of 86%, and the Kappa coefficient was 0.76. The accuracy of the model in this study was quite good. Lukas et al., using the CA-ANN model, gave slightly good accuracy and a Kappa coefficient at 86.5% and 0.82, respectively [23]. Xiong et al. used CA-Markov and LCM (Land Change Modeler) models and obtained Kappa coefficients of 0.82 and 0.78, slightly higher than that of this study's CA-ANN model [19]. When the Kappa coefficient is greater than 0.75, the model is a good predictor [19]. Therefore, the CA-ANN model applied in this study is suitable for simulating the LULC change map.

The simulated LULC map for 2033 and the area are shown in Fig. 6 and Fig. 7. The Dense vegetation is forecasted to be 673.5 km^2, decreasing by 2% compared with 2023. In contrast, Sparse vegetation and Built-up area extend by 1.3% (376.2 km^2) and 0.5% (41.0 km^2), respectively. The Bare land and Water bodies are also forecasted to increase slightly, with 47.8 km^2 and 13.1 km^2 (0.1% for each class).

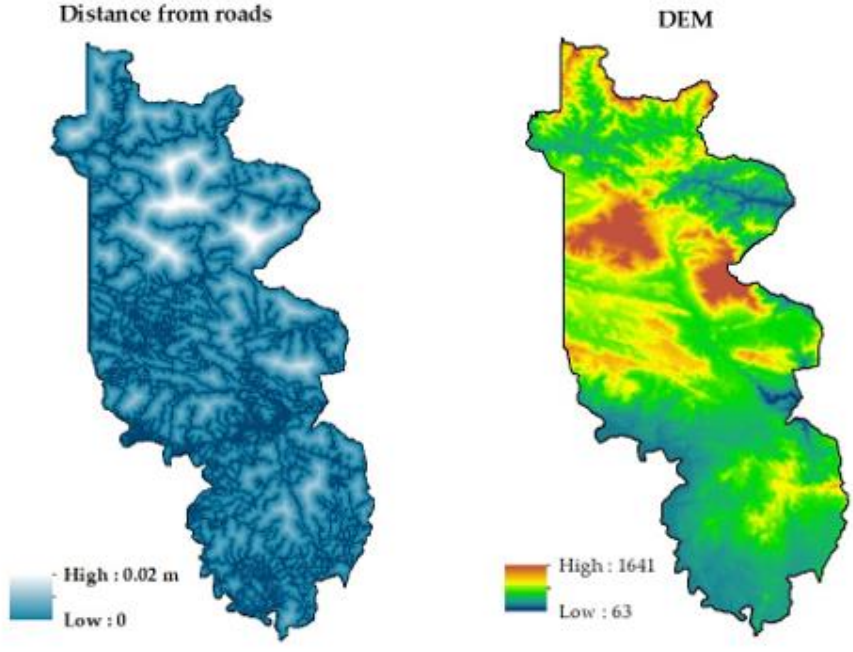

Fig. 5. Map of distance from road and DEM

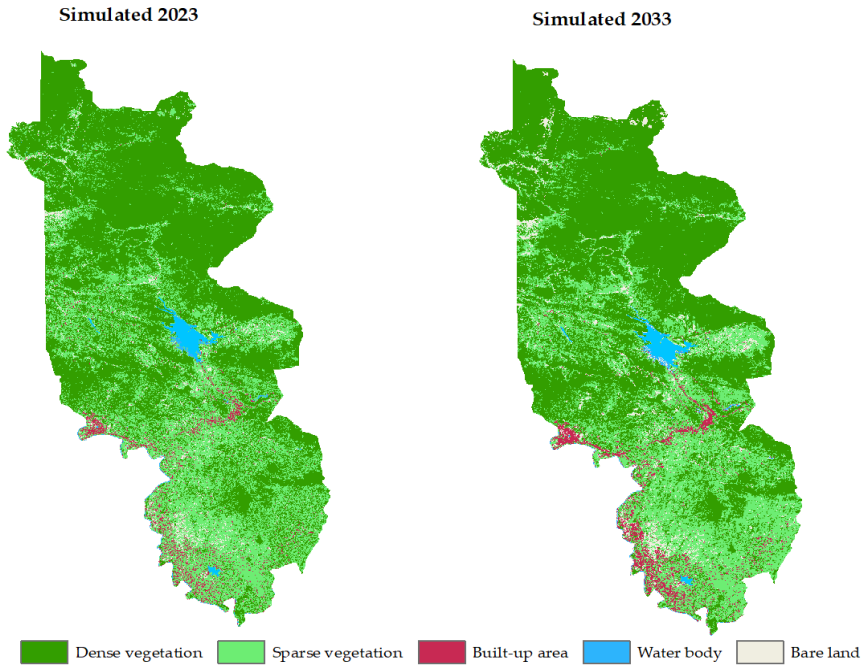

Fig. 6. Simulated LULC map for 2023 and 2033

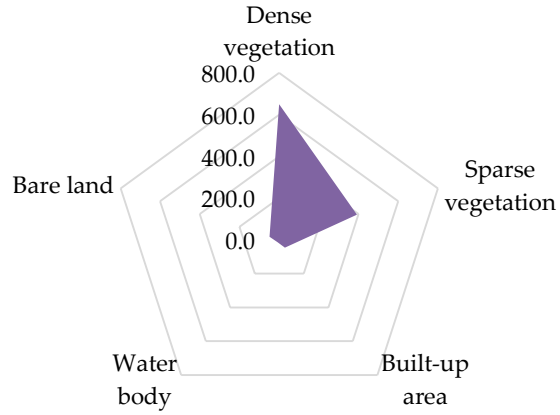

Fig. 7. Simulated LULC area for 2033 (km^2)

4 Conclusion

In this study, we built LULC maps for 2013, 2018, and 2023 by interpreting remote-sensing images with the MLC method. They had good accuracy, with Kappa coefficients of 0.82–0.85. The total area is 1,151.8 km^2. The LULC change in the 10-year period from 2013 to 2023 included a 1.4% decrease in Dense vegetation due to transferring to Sparse vegetation. Similarly, the Built-up area decreased by 0.6%. Meanwhile, Sparse vegetation, Bare land, and Water bodies increased by 1.3, 0.5, and 0.2%, respectively. The simulated LULC change for 2033 with the CA-ANN algorithm in the QGIS MOLUSCE plugin had relatively good results, with an overall accuracy of 86% and a Kappa coefficient of 0.76. This model is suitable for predicting the LULC change for 2033. By 2033, Dense vegetation was forecasted to decrease by 2% compared with that of 2023. Sparse vegetation and Built-up area increase by 1.3 and 0.5%, respectively. Water bodies and Bare land were predicted to increase by 0.1% for each.

Funding

This research was funded by the Vietnam Ministry of Education and Training, under Grant B2022-DHH-16.

References

1. Sudhakar, S. & Kameshwara, R. (2010), Land Use and Land Cover Analysis, in Roy, P. S., Dwivedi, R. S. and Vijayan (Ed.), D., *Remote Sensing Applications*, NRSC.
2. Government of Canada, *Land Cover/Biomass Mapping*. https://www.nrcan.gc.ca/maps-tools-and-publications/satellite-imagery-and-air-photos/tutorial-fundamentals-remote-sensing/educational-resources-applications/land-cover-biomass-mapping/land-cover-land-use/9373, Accessed 12 May 2023.
3. EPA (2012), *Impacts of changes in land use and land cover on U.S*, Air quality: Development and application of an integrated climate-vegetation-chemistry modeling system. http://cfpub.epa.gov/si/si_public_comments.cfm.
4. Shahrin, N. N., Asmat, A., Hazali, N. A., Sahak, N. (2019), Land use and land cover (LULC) modification on the climate and air quality variations, *IOP Conf. Ser.: Earth Environ. Sci.*, 373 012009. https://doi.org/10.1088/1755-1315/373/1/012009.
5. Rawat, J. S. & Kumar, M. (2015), Monitoring land use/cover change using remote sensing and GIS techniques: A case study of Hawalbagh block, district Almora, Uttarakhand, India *The Egyptian Journal of Remote Sensing and Space Science*, 18(1), 77–84. https://doi.org/10.1016/j.ejrs.2015.02.002.

6. Alshari, E. A. & Gawali, B. W. (2021), *Development of classification system for LULC using remote sensing and GIS. Global Transitions Proceedings*, 2(1), 8–17. https://doi.org/10.1016/j.gltp.2021.01.002.
7. Samal, D. R. & Gedam, S. S. (2015), Optimal ground control points for geometric correction using genetic algorithm with global accuracy, *Eur. J. Remote Sens.*, 48, 85–99.
8. Wubie, M. A., Assen, M., Nicolau, M. D. (2016), Patterns, causes and consequences of land use / cover dynamics in the Gumara watershed of lake Tana basin, Northwestern Ethiopia, *Environ. Syst. Res.*, 5, 1–12.
9. Mishra, V. N., Prasad, R., Kumar, P., Gupta, D. K., Dikshit, P. K. S., Dwivedi, S., Singh, R. S., Srivastava, V. (2015), Supervised Algorithms for Classification of Remotely Sensed Satellite Image using Open Source Support, Conference: *National Conference on Open Source GIS: Opportunities and Challenges,* Department of Civil Engineering, IIT (BHU), Varanasi.
10. Norovsuren, B., Tseveen, B., Batomunkuev, V., Renchin, T., Natsagdorj, E., Yangiv, A., Mart, Z. (2019), Land cover classification using maximum likelihood method (2000 and 2019) at Khandgait valley in Mongolia, *IOP Conf. Ser.: Earth Environ. Sci*., 381, 012054. https://doi.org/10.1088/1755-1315/381/1/012054.
11. Seyam, Md. M. H., Haque, Md. R., Rahman, Md. M. (2023), Identifying the land use land cover (LULC) changes using remote sensing and GIS approach: A case study at Bhaluka in Mymensingh, Bangladesh, *Case Studies in Chemical and Environmental Engineering,* 7, 100293.
12. Kamaraj, M. & Rangarajan, S. (2022), Predicting the Future Land Use and Land Cover Changes for Bhavani Basin, Tamil Nadu, India Using QGIS MOLUSCE Plugin, *Environmental Science and Pollution Research*, 29, 86337–86348.
13. People's Committee of Huong Hoa district (2022), Report on implementation of Socio-economic Development Tasks in 2022 and Socio-economic Development Plan in 2023, Huong Hoa district.
14. ArcGIS Desktop 9.3 Help (2011), *How Maximum Likelihood Classification works*. https://webhelp.esri.com/arcgisdesktop/9.3/index.cfm?TopicName=How%20Maximum%20Likelihood%20Classification%20works. (Accessed 12 May 2023).
15. Richards, J. A. (1986), *Remote Sensing Digital Image Analysis*, 173–189. https://doi.org/10.1007/978-3-662-02462-1_8.
16. Liang, S., Cheng, J., Zhang, J. (2020), Maximum likelihood classification of soil remote sensing image based on deep learning, *Earth Sci. Res. J.*, 24(3), 357–365. https://doi.org/10.15446/esrj.v24n3.89750.

17. ESRI (2021), Compute Confusion Matrix. https://desktop.arcgis.com/en/arcmap/latest/tools/spatial-analyst-toolbox/compute-confusion-matrix.htm. (Accessed 20/5/2023).

18. Leta, M. K., Demissie, T. A., Tränckner, J. (2021), Modeling and Prediction of Land Use Land Cover Change Dynamics Based on Land Change Modeler (LCM) in Nashe Watershed, Upper Blue Nile Basin, Ethiopia, *Sustainability*, 13(7), 3740. https://doi.org/10.3390/su13073740.

19. Xiong, N., Yu, R., Yan, F., Wang, J. & Feng, Z. (2022), Land use and Land cover changes and prediction based on Multi-Scenario Simulation: A case study of Qishan County, China. *Remote Sensing*, 14(16), 4041.

20. Muhammad, R., Zhang, W., Abbas, Z., Guo, F., Gwiazdzinski, L. (2022), Spatiotemporal Change Analysis and Prediction of Future Land Use and Land Cover Changes Using QGIS MOLUSCE Plugin and Remote Sensing Big Data: A Case Study of Linyi, China, *Land*, 11(3), 419. https://doi.org/10.3390/land11030419.

21. Abbas, Z. & Jaber, H. S. (2020), Accuracy assessment of supervised classification methods for extraction land use maps using remote sensing and GIS techniques, *IOP Conf. Ser.: Mater. Sci. Eng.*, 745, 012166. https://doi.org/10.1088/1757-899X/745/1/012166.

22. People's Committee of Huong Hoa district (2022), Report on Current Land Use Status in Huong Hoa district, Quang Tri province in 2022.

23. Lukas, P., Melesse, A. M., Kenea, T. T. (2023), Prediction of Future Land Use/Land Cover Changes Using a Coupled CA-ANN Model in the Upper Omo–Gibe River Basin, Ethiopia, *Remote Sens.*, 15(4), 1148. https://doi.org/10.3390/rs15041148.